

Magnetization Estimation From MFM Images

Chi-Chun Hsu, *Member, IEEE*, Clayton T. Miller, *Member, IEEE*, Ronald S. Indeck, *Senior Member, IEEE*, Joseph A. O'Sullivan, *Senior Member, IEEE*, and Marcel W. Muller, *Life Fellow, IEEE*

Abstract—We have developed a method to estimate the *complete magnetization in thin-film longitudinal recording media from magnetic force microscopy (MFM) data. The method uses a medium model described by a Voronoi tessellation of the film plane. The magnetization lies in that plane, has constant magnitude, and is uniform within each convex region, or grain, of the tessellation. The effect of a single grain on the MFM simulation is isolated by considering the difference between the MFM images before and after that grain undergoes a 180° magnetization reversal. Using this difference image, the complete magnetization of the grain and the grain's boundaries are estimated. By isolating each grain in turn, as if a series of incremental applied fields had been applied, the magnetization for the whole pattern is estimated.*

Index Terms—Irrotational and solenoidal components, magnetization reversal, magnetic force microscopy (MFM), Voronoi tessellation.

I. INTRODUCTION

A THOROUGH understanding of the storage capacity and environmental and temporal stability of thin-film longitudinal magnetic storage media requires knowledge of their physical and magnetic microstructure, most importantly a detailed map of the magnetization. This mapping can be carried out using electron microscopy, but this method requires elaborate sample preparation and a vacuum. It would be much more convenient to use magnetic force microscopy (MFM) images to estimate the magnetization $\mathbf{M}(x, z)$, where x and z are the film plane variables and the magnetization is assumed to lie in this plane. MFM offers the advantages of easy sample preparation, a measurement under ambient conditions, high resolution, and simultaneous topographic mapping. The problem with reconstructing $\mathbf{M}(x, z)$ from MFM data is that MFM measurements only depend upon part of the magnetization. The Helmholtz theorem allows $\mathbf{M}(x, z)$ to be decomposed into the sum of an irrotational component $\mathbf{M}^d(x, z)$ and a solenoidal component $\mathbf{M}^c(x, z)$, where

$$\begin{aligned}\nabla \cdot \mathbf{M}(x, z) &= \nabla \cdot \mathbf{M}^d(x, z) \\ \nabla \times \mathbf{M}(x, z) &= \nabla \times \mathbf{M}^c(x, z)\end{aligned}$$

and

$$\nabla \times \mathbf{M}^d(x, z) = \nabla \cdot \mathbf{M}^c(x, z) = 0.$$

An MFM image alone cannot give any information about $\mathbf{M}^c(x, z)$ because this component of the magnetization creates

no external fields for the MFM to sense. However, if the MFM data are combined with the assumption that thin-film longitudinal media are well modeled by a Voronoi tessellation of the film plane, where $\mathbf{M}(x, z)$ has a constant magnitude and is uniform within the tessellation grains [1], then estimating $\mathbf{M}^c(x, z)$ becomes more feasible. The restrictions placed on $\mathbf{M}(x, z)$ by this model and by most conventional micromagnetic models provide an advantage that will be illustrated with simulations.

II. MFM IMAGE SIMULATION AND $\mathbf{M}^d(x, z)$ RECONSTRUCTION

Consider MFM images gathered in the resonant detection mode with a perpendicularly magnetized tip. Such measurements are roughly proportional to the second derivative with respect to y of $H_y(x, y, z)$, the component of magnetic field perpendicular to the film plane [2]. As the MFM tip scans across the medium surface, it maps out an image of this second derivative at a fixed height y_{tip} above the medium. Modeling MFM data therefore involves calculating $H_y(x, y_{\text{tip}}, z)$ from some underlying magnetization $\mathbf{M}(x, z)$. Consider a magnetic film of thickness δ lying between the planes defined by $y = \pm\delta/2$. If $\mathbf{M}(x, z)$ for the film has no y component and is invariant in the y direction, then [3]

$$\begin{aligned}\frac{\partial^2 H_y(\mathbf{K}, y_{\text{tip}} > \delta/2)}{\partial y^2} \\ = -iK \sinh\left(\frac{K\delta}{2}\right) e^{-Ky_{\text{tip}}} (\mathbf{K} \cdot \mathbf{M}(\mathbf{K}))\end{aligned}\quad (1)$$

where the left side is the second derivative with respect to y of the two-dimensional (2-D) Fourier transform of $H_y(x, y_{\text{tip}}, z)$. The transform is with respect to the in-plane coordinates x and z . The vector \mathbf{K} is defined as $\mathbf{K} \equiv \mathbf{x}k_x + \mathbf{z}k_z$, where \mathbf{x} and \mathbf{z} are unit vectors and k_x and k_z are the spatial frequency variables. $K = |\mathbf{K}|$, and $\mathbf{M}(\mathbf{K})$ is the 2-D Fourier transform of $\mathbf{M}(x, z)$. Since $i\mathbf{K} \cdot \mathbf{M}(\mathbf{K})$ is the 2-D transform of $\nabla \cdot \mathbf{M}(x, z)$, (1) illustrates that MFM images depend only upon $\mathbf{M}^d(x, z)$.

The reconstruction of $\mathbf{M}^d(x, z)$ from an MFM image is obtained from the inverse 2-D Fourier transform of [3]

$$\mathbf{M}^d(\mathbf{K}) = \frac{i\mathbf{K}e^{Ky_{\text{tip}}}}{K^3 \sinh\left(\frac{K\delta}{2}\right)} \frac{\partial^2 H_y(\mathbf{K}, y_{\text{tip}} > \delta/2)}{\partial y^2}.\quad (2)$$

Fig. 1 illustrates the use of (1) for the simulation of an MFM image from $\mathbf{M}(x, z)$ and (2) for the reconstruction of $\mathbf{M}^d(x, z)$ from the simulated MFM image.

Manuscript received February 15, 2001; revised May 28, 2002. This work was supported in part by the National Science Foundation under Grants ECS-0000434 and ECS-9900159.

The authors are with the Magnetism and Information Science Center, Department of Electrical Engineering, Washington University, St. Louis, MO 63130 USA (email: rsi@ee.wustl.edu).

Digital Object Identifier 10.1109/TMAG.2002.803586.

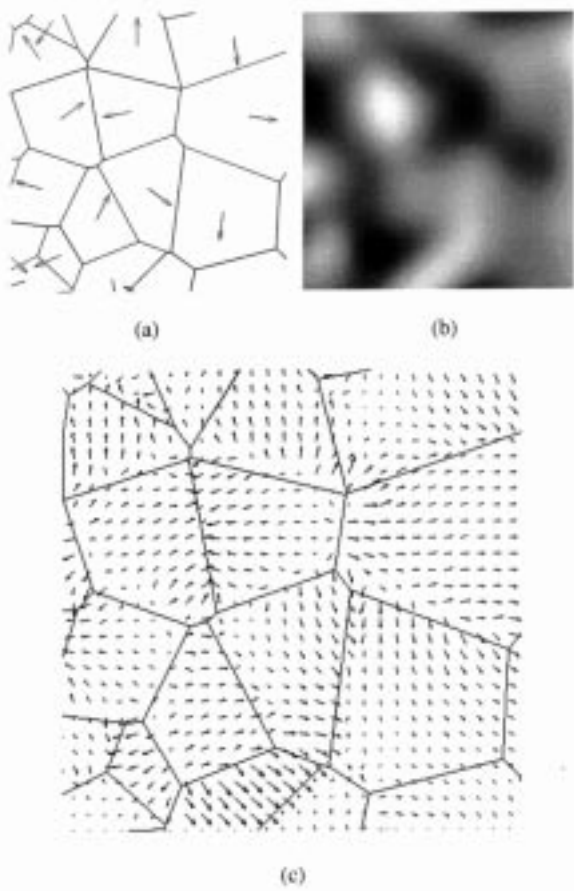


Fig. 1. Illustration of MFM simulation and reconstruction of $\mathbf{M}^d(x, z)$. (a) Simulated $0.9 \mu\text{m} \times 0.9 \mu\text{m}$ magnetization pattern with $\delta = 50 \text{ nm}$. (b) Corresponding MFM image generated according to (1), with $y_{\text{tip}} = 200 \text{ nm}$. (c) Reconstruction of $\mathbf{M}^d(x, z)$ according to (2).

III. CONSTRAINED RECONSTRUCTION OF $\mathbf{M}^c(x, z)$

Let a single grain in the pattern reverse its magnetization 180° , and capture MFM images before and after this flip. The difference between these two MFM images isolates the effects of the flipped grain [4], [5]. Applying the reconstruction algorithm to the difference MFM image results in the irrotational field associated with the flipped grain only. This procedure is illustrated in Fig. 2. Fig. 2(b) shows the irrotational field associated with the single flipped grain along with that grain's boundaries. Let this field now be \mathbf{M}^d , and let \mathbf{M} now refer to the isolated grain's complete, unknown magnetization. Decompose \mathbf{M} into the sum of \mathbf{M}_{in} and \mathbf{M}_{out} . \mathbf{M}_{in} equals \mathbf{M} inside the grain and is zero outside, while \mathbf{M}_{out} equals \mathbf{M} outside the grain and is zero inside. Write \mathbf{M}_{in} as the sum of \mathbf{M}_{in}^d and \mathbf{M}_{in}^c , and similarly for \mathbf{M}_{out} . Because a single grain has been isolated, \mathbf{M}_{out} is zero. However, $\mathbf{M}_{\text{out}}^d$ and $\mathbf{M}_{\text{out}}^c$ are nonzero. The fact that $\mathbf{M}_{\text{out}} = \mathbf{M}_{\text{out}}^d + \mathbf{M}_{\text{out}}^c = 0$ leads to $\mathbf{M}_{\text{out}}^c = -\mathbf{M}_{\text{out}}^d$. The only missing piece is \mathbf{M}_{in}^c .

The model constrains the magnetization within a grain to be a uniform vector field \mathbf{M} in the x - z plane. The procedure for finding \mathbf{M}_{in}^c begins with making a guess at \mathbf{M} , called \mathbf{M}_{est} . The estimate for \mathbf{M}_{in}^c is then $\mathbf{M}_{\text{inest}}^c = \mathbf{M}_{\text{est}} - \mathbf{M}_{\text{in}}^d$, and $\mathbf{M}_{\text{est}}^c = \mathbf{M}_{\text{inest}}^c + \mathbf{M}_{\text{out}}^c$. $\mathbf{M}_{\text{est}}^c$ is tested to see whether or not it

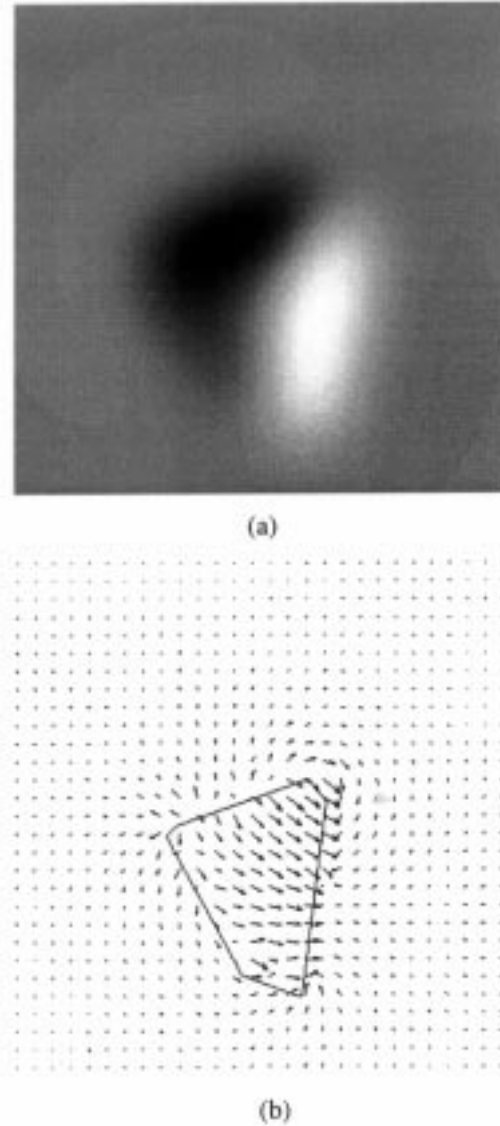


Fig. 2. (a) Difference between MFM image simulations taken before and after a single grain flips its magnetization. (b) Reconstruction applied to the difference image, resulting in the part of \mathbf{M}^d associated with the flipped grain.

is purely a rotational field. This is done by substituting it into (1) to simulate the MFM's response to the estimated pattern. If the guess at the magnetization was accurate, then $\mathbf{M}_{\text{est}}^c$ is solenoidal and the simulated output image has very little contrast because MFM is not sensitive to solenoidal patterns. If the image has a lot of contrast, $\mathbf{M}_{\text{est}}^c$ is not solenoidal and another guess is made at \mathbf{M} . An iterative procedure finds the \mathbf{M} that minimizes the amount of energy, defined as the sum of the squared pixel values, in the simulated MFM image of $\mathbf{M}_{\text{est}}^c$.

This estimation process can be carried out grain by grain in order to estimate the magnetization of the entire region. The estimates for the individual grains are simply summed.

IV. ESTIMATING GRAIN BOUNDARIES

In order to apply this approach, knowledge of grain boundaries is required. The grain boundaries are estimated using the divergence of \mathbf{M}^d associated with a single flipped grain. Since

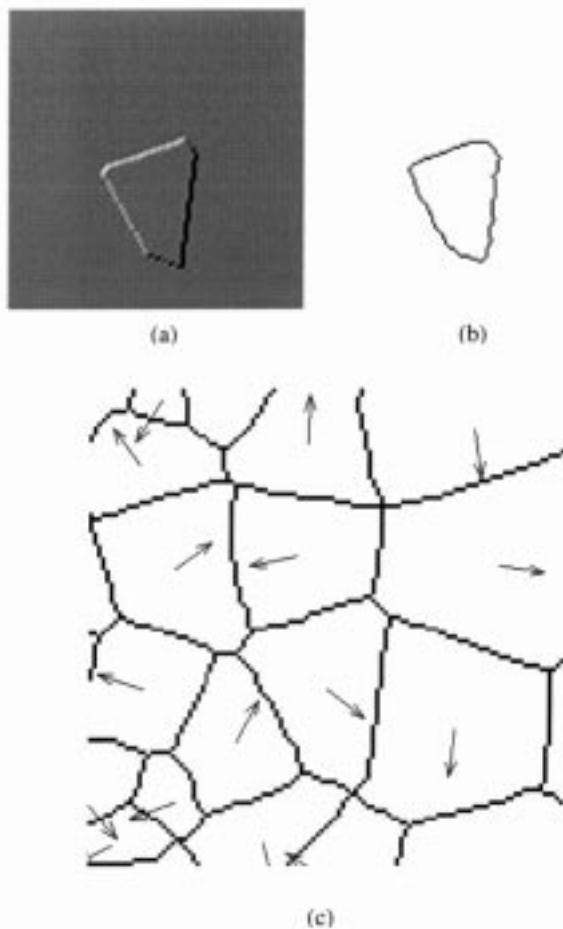


Fig. 3. A grain's boundaries are detected by computing the divergence of the reconstructed M^d fields. (a) The divergence of M^d from Fig. 2(b). (b) The edge detected grain boundary. (c) The complete reconstruction performed without using knowledge of the grain boundaries.

$\nabla \cdot \mathbf{M} = \nabla \cdot \mathbf{M}^d$, and \mathbf{M} consists of uniformly magnetized grains, we expect large values of $\nabla \cdot \mathbf{M}^d$ to correspond to the discontinuities in the magnetization at grain edges. Fig. 3(a) is a gray scale image of the divergence of the pattern shown in Fig. 2(b) and the edges of the grain are outlined.

In order to automatically find grain boundaries from an image like Fig. 3(a), we first perform edge detection upon the image using the Sobel method implemented in MATLAB[®]. The resulting edges are further refined with morphological operations from the MATLAB[®] image processing toolbox. The final product is shown in Fig. 3(b).

This boundary detection process is performed on each of the grains shown in Fig. 1(a). First, the 180° reversal is used to generate a difference image that is then reconstructed to find the M^d associated with each grain. Then $\nabla \cdot \mathbf{M}^d$ is computed and processed as discussed to find the grain boundaries. Finally, these

boundaries are used in the reconstruction process described in Section III, resulting in Fig. 3(c).

V. DISCUSSION AND CONCLUSION

In 1989, Beardsley showed how to reconstruct the irrotational component of the magnetization in thin-film longitudinal media from external field measurements such as those obtained by recording or MFM measurements. Similar experimental reconstructions have been made by treating an MFM image as the convolution of a tip dipole response function with a magnetization pattern. Measured dipole response functions can then be used to reconstruct the irrotational component of magnetization from the MFM image [6]. In order to reconstruct the entire magnetization, additional information about or constraints on the magnetization must be available. We describe a novel method for reconstructing the complete magnetization for a longitudinal recording medium by imposing constraints on it. First, the magnetization lies in the plane of the film and its magnitude is the same at every point in the film. Second, the magnetization is uniform within individual grains that form a tessellation of the film plane. Third, the individual grains sequentially reverse their magnetization. Using these constraints and a model for the MFM, the tessellation and magnetization are estimated.

While grains in real thin-film longitudinal media may not behave in the orderly fashion that simplifies the reconstruction process demonstrated here, it is possible to use MFM to observe granular switching behavior [2], [4], [5]. This is accomplished by making MFM images of the same region at different remanent states. The difference between the images of nearby remanent states will highlight those clumps of grains whose magnetizations have flipped. Our plan is to further develop the methodology described here and apply it to these difference images to enable full magnetization estimation from real MFM measurements.

REFERENCES

- [1] D. G. Porter *et al.*, "Irregular grain structure in micromagnetic simulation," *J. Appl. Phys.*, vol. 79, no. 8, April 15, 1996.
- [2] A. Jander, "Texture induced variations in switching fields of hard disk media investigated by magnetic force microscopy," Ph.D. dissertation, Washington Univ., St. Louis, MO, 1999.
- [3] I. A. Beardsley, "Reconstruction of the magnetization in a thin film by a combination of Lorentz microscopy and external field measurements," *IEEE Trans. Magn.*, vol. 25, pp. 671–677, Jan. 1989.
- [4] A. Jander, P. Dhagat, R. S. Indeck, and M. W. Muller, "MFM observation of localized demagnetization in magnetic recordings," *IEEE Trans. Magn.*, vol. 34, pp. 1657–1659, July 1998.
- [5] C.-C. Hsu *et al.*, "MFM observation of magnetization reversal process in recording media with lithographically defined texture," *IEEE Trans. Magn.*, vol. 36, pp. 2327–2329, Sept. 2000.
- [6] R. Madabhushi, R. D. Gomez, E. R. Burke, and I. D. Mayergoyz, "Magnetic biasing and MFM image reconstruction," *IEEE Trans. Magn.*, vol. 32, pp. 4147–4149, Sept. 1996.